J|A|C|S
ARTICLES
Published on Web 10/20/2004

Relationship of Stereochemical and Skeletal Diversity of Small Molecules to Cellular Measurement Space

Young-kwon Kim,[†,‡,§] Midori A. Arai,[†,‡] Takayoshi Arai,[†,‡] Julia O. Lamenzo,[§] Elton F. Dean, III,[§] Nick Patterson,[§] Paul A. Clemons,*[,‡,§] and Stuart L. Schreiber*[,†,‡,§]

Contribution from the Howard Hughes Medical Institute, Department of Chemistry and Chemical Biology, and The Eli and Edythe Broad Institute, Program in Chemical Biology, Harvard University, 12 Oxford Street, Cambridge, Massachusetts 02138

Received March 30, 2004; E-mail: pclemons@hms.harvard.edu; stuart_schreiber@harvard.edu

Abstract: Systematic and quantitative measurements of the roles of stereochemistry and skeleton-dependent conformational restriction were made using multidimensional screening. We first used diversity-oriented synthesis to synthesize the same number (122) of [10.4.0] bicyclic products (**B**) and their corresponding monocyclic precursors (**M**). We measured the ability of these compounds to modulate a broad swath of biology using 40 parallel cell-based assays. We analyzed the results using statistical methods that revealed illuminating relationships between stereochemistry, ring number, and assay outcomes. Conformational restriction by ring-closing metathesis increased the specificity of responses among active compounds and was the dominant factor in global activity patterns. Hierarchical clustering also revealed that stereochemistry was a second dominant factor; whereas the stereochemistry of macrocyclic appendages was a determinant for bicyclic compounds, the stereochemistry of the carbohydrates was a determinant for the monocyclic compounds of global activity patterns. These studies illustrate a quantitative method for measuring stereochemical and skeletal diversity of small molecules and their cellular consequences.

Introduction

The roles of stereochemistry and skeleton-based conformational constraints on the performance of small molecules in biological assays can be intuited, but systematic and quantitative measurements are lacking. Here we describe the use of diversity-oriented synthesis (DOS),[1] multidimensional screening,[2] and statistical and clustering analyses to achieve this goal. The results, which reveal striking relationships, provide an explicit illustration of how reagent selection in DOS can be predicted to effect subsequent biological outcomes involving the resultant products. This approach may facilitate an understanding of relationships between chemical descriptor space and biological measurement space (Figure 1).[3]

Our plan involved the synthesis of a collection of carbohydrate-derived small molecules differing in stereochemistry and having two appendages that are either joined at their termini to form a 12-membered ring or not (Figure 2a). We chose a 12-membered ring-forming reaction yielding macrolides having hexagonal shapes[4] in order to assess the influence of stereochemistry and macrocycle-based conformational constraints on biological activities. We measured the latter using multidimensional screening,[5] (Figure 1) in which both precursor monocycles (**M**) and their bicyclic products (**B**) were included in a three-dimensional matrix of biological measurements whose axes represent small molecules, a panel of four cell-based assay measurements, and a panel of 18 cell states imposed by exposing screening cell cultures to a collection of 17 known small-molecule modulators of biological response (i.e., chemical-genetic modifier screens[6]) or not (Figure 2b). To allow test compounds maximal opportunity to perturb cell-based assays, cellular assay measurements were chosen that report on broad biological processes, rather than on highly targeted pathway- or protein-specific events (Figure 2c). In contrast to conventional, one-dimensional small-molecule screens, in which a compound collection is typically exposed to a single set of assay conditions, this approach results in vectors of measured values

[†] Howard Hughes Medical Institute.
[‡] Department of Chemistry and Chemical Biology.
[§] The Eli and Edythe Broad Institute.

(1) (a) Schreiber, S. L. *Science* **2000**, *287*, 1964−1969. (b) Burke, M. D.; Schreiber, S. L. *Angew. Chem., Int. Ed.* **2004**, *43*, 46−58.
(2) Haggarty, S. J.; Koeller, K. M.; Wong, J. C.; Butcher, R. A.; Schreiber, S. L. *Chem. Biol*. **2003**, *10*, 383−396.
(3) (a) Schreiber, S. L. *Chem. Eng. News* **2003**, *81*, 51−61. (b) Strausberg, R. L.; Schreiber, S. L. *Science* **2003**, *300*, 294−295.
(4) Lee, D.; Sello, J. K.; Schreiber, S. L. *J. Am. Chem. Soc*. **1999**, *121*, 10648−10649.
(5) See Supporting Information (Section V) for a description of multidimensional screening and data analysis methods. A detailed description of multidimensional screening (including conceptual basis, detailed assay development and error-modeling methods, and role in hypothesis-generation) will be presented elsewhere: Lamenzo, J. O.; Dean, E. F.; Gorenstein, J.; Kim, Y.-K.; Wagner, B. K.; Schreiber, S. L.; Clemons, P. A. Manuscript in preparation.
(6) Koeller, K. M.; Haggarty, S. J.; Perkins, B. D.; Leykin, I.; Wong, J. C.; Kao, M.-C. J.; Schreiber, S. L. *Chem. Biol*. **2003**, *10*, 397−410.

10.1021/ja048170p CCC: $27.50

multidimensional screening	the use of high-throughput screening to perform parallel experiments exposing a common small-molecule collection to combinations of experimental variables (*e.g.*, multiple assay readouts, cell states, or time- and/or dose-response series); designed to discover dependencies between such experimental variables
biological measurement space	a metric (*e.g.*, vector) space defined by an ordered collection of empirical biological measurements, such as obtained by multidimensional screening
chemical-genetic fingerprint	an individual vector (*i.e.*, position) in a biological measurement space destined for chemical-genetic analysis; corresponds to global performance of a single small-molecule across an ordered set of biological assays
chemical descriptor space	a metric (*e.g.*, vector) space defined by a collection of computed or predicted values calculated for each member of a common small-molecule collection
clustering analysis	a general technique in global analysis. applied using an appropriate distance metric to a collection of objects in a metric space; aims to assign objects to groups (*i.e.*, clusters) on the basis of relative similarity

Figure 1. Glossary of terms relating experimental design and data analysis.

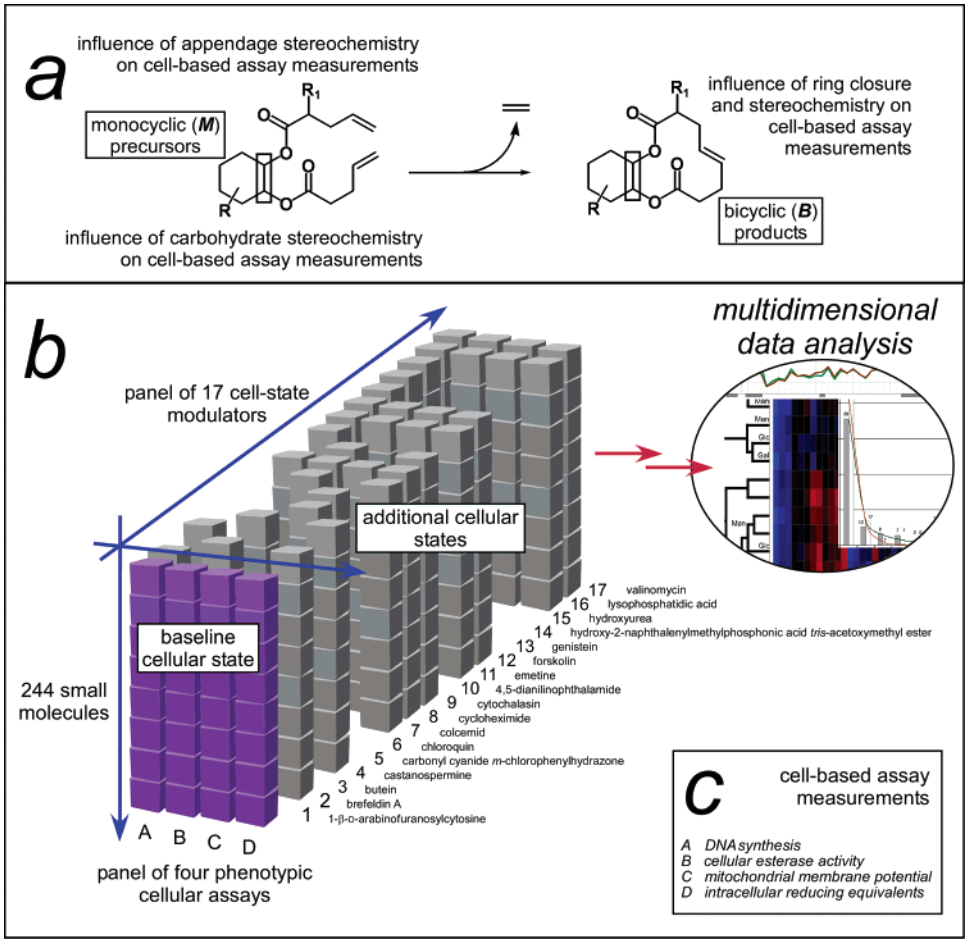

Figure 2. Experimental design to test roles of stereochemistry and ring closure on biological activities by multidimensional screening. (a) Structural variability present in test library members due to appendages, carbohydrates, and ring closure. (b) Variables in multidimensional screening experiment, illustrating the generation of a data matrix amenable to multidimensional data analysis. (c) Cell-based assay measurements chosen to provide broad biological interrogation.

for each compound and is formally analogous to other types of profiling experiments, such as transcriptional or metabolic profiling.

To analyze the results of these experiments, we took two approaches. First, we grouped compounds from each of the **M** and **B** compound classes according to the number of assays in which each compound scored as positive. The resulting frequency distributions were analyzed using a novel statistical test that allowed experimental results to be compared to the results of random permutation testing. This method allowed an explicit statistical statement about the likelihood of observing our results by chance. Second, we categorized compounds according to stereochemical descriptors and computed average chemical-genetic fingerprints for each category that encode their performance in a multidimensional biological measurement space. This method allowed the application of clustering analysis, specifically hierarchical clustering, to uncover relationships between stereochemical and skeletal elements in determining biological performance (Figure 1).

Results and Discussion

Efficiency of Macrocyclic Ring-Closing Metathesis on Model Substrates. We first determined reactivity patterns of carbohydrate-based substrates when exposed to ring-forming reactions. For ring-closing metathesis (RCM) reactions, α-substituents on the unsaturated ester appendages, independent of their relative stereochemistry, have only minor effects on rates and yields (Figure 3; **1b**, **1c**); however, allylic and vinylic substitutions dramatically decrease the rate of ring closure (data not shown). The carbohydrate-based six-membered ring

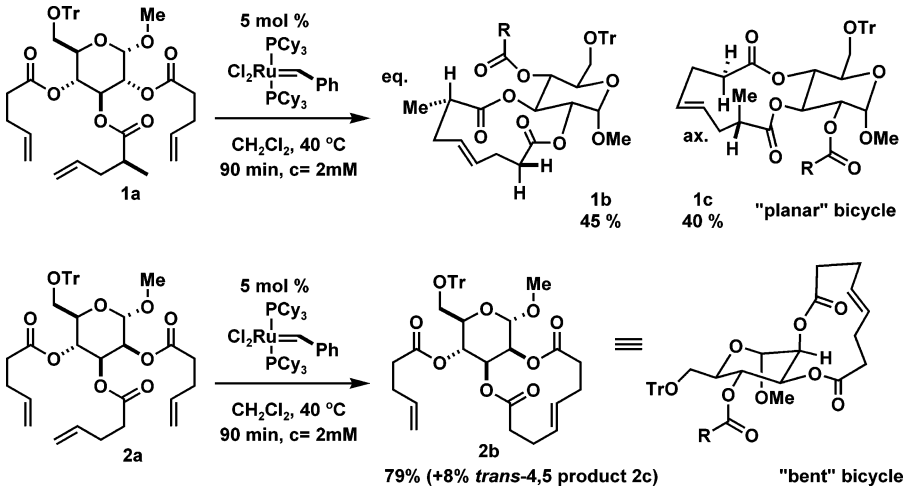

Figure 3. Role of stereochemistry in ring closure. *Trans*-stereochemistry of unsaturated diesters results in a ring-closing reaction yielding a "planar" bicycle; *cis*- (versus *trans*-) stereochemistry provides faster cyclization and results in a "bent" bicycle.

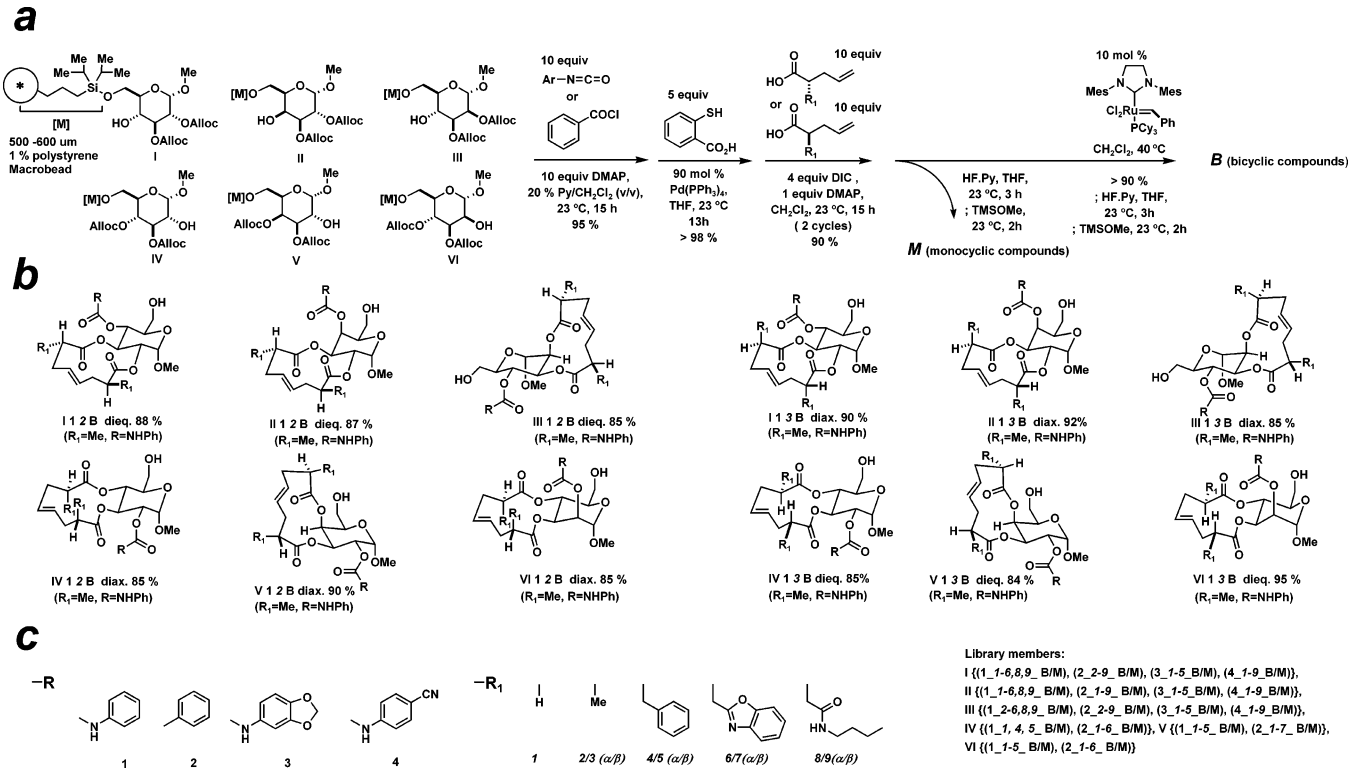

Figure 4. Synthesis of test library of monocyclic and bicyclic compounds. (a) 5 mM DMSO stock solutions of the illustrated 122 bicyclic products (**B**) and their 122 monocyclic precursors (**M**, structures not shown) were prepared as indicated, affording (b) products, each as nearly a single entity;[9b] three-dimensional renderings are based on X-ray structure determination for analogous compounds. (c) Numbered building-block fragments corresponding to superatoms **R** and $\mathbf{R_1}$ and encoded designations of products found in the completed library.

increases the overall efficiency of the ring closure regardless of its ring elements and substitution patterns. Internal competitive ring closure of mannose-derived tris-unsaturated ester **2a** revealed that *cis*-fused, conformationally constrained bicyclic product **2b** (79%) forms more rapidly than *trans*-fused product **2c** (8%). Our reactivity studies also indicate that the ring closures are irreversible under the conditions used.[7]

Library Synthesis. We next developed a DOS pathway yielding 244 compounds, 122 having two acyclic, unsaturated ester appendages, and 122 having an appended, 12-membered ring resulting from joining the two terminal olefins by RCM (Figure 4). In principle, all possible combinations of reagent selections could have yielded 432 products. However, we synthesized and screened only the 122 pairs of compounds shown here, primarily due to the efficiency of the chemical transformations. Six differentially bis-protected carbohydrate-derived diols were synthesized in several steps from commercially available, inexpensive starting materials[8] and attached selectively to macrobeads (Figure 4; **I**−**VI**, ca. 90 nmol/bead).[9] Each set of macrobead-bound substrates was divided into four

(7) (a) Resubmission of each pure product to the reaction conditions did not yield the other product. (b) The galactose-based triene showed the same preference for *cis*-fused product formation.

(8) Diols were synthesized in two to five steps from commercially available starting materials (<$5/g), proceeding in overall yields of 40−75%.

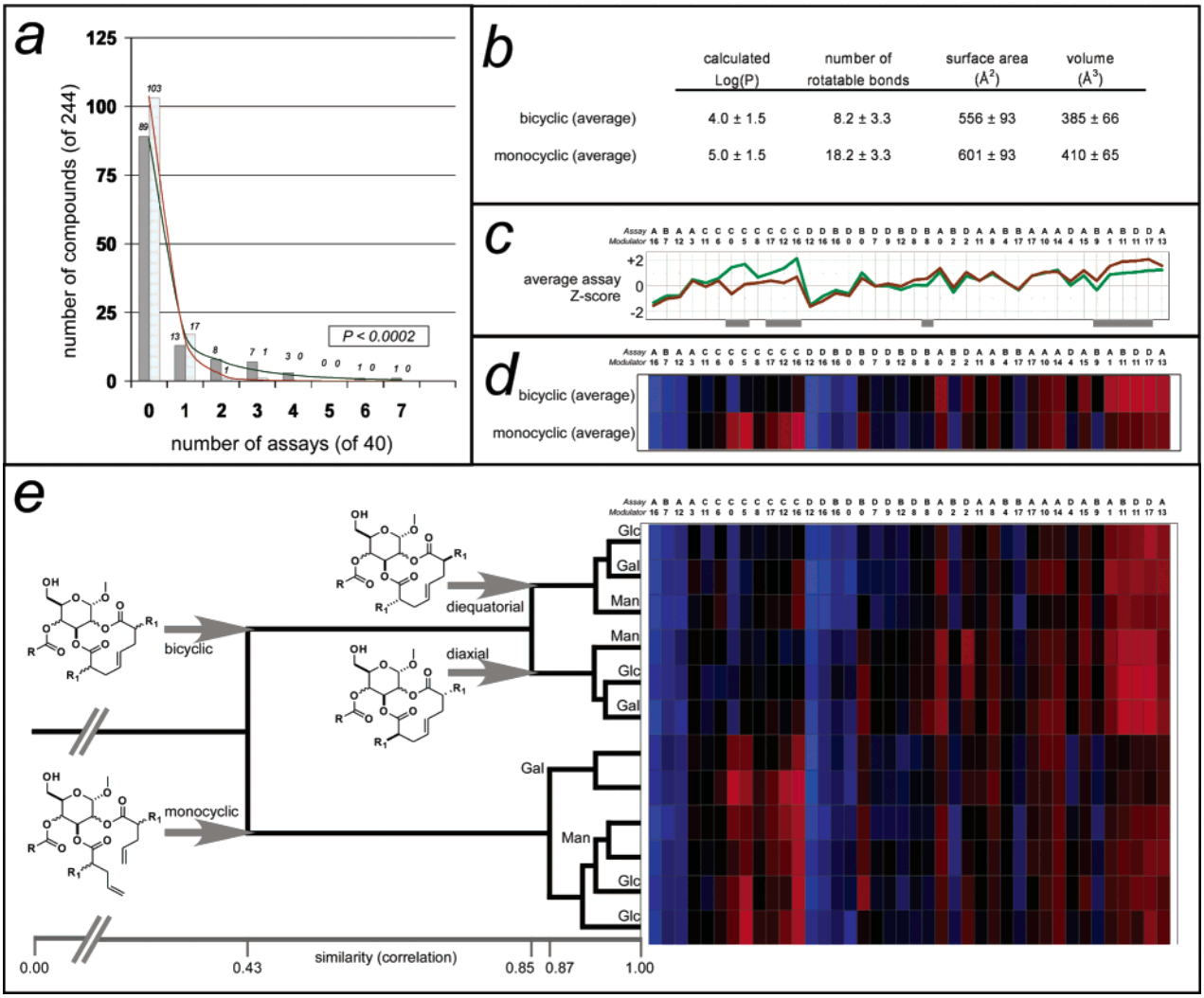

Figure 5. Global analysis of outcomes in biological measurement space. Codes for assay readouts (**A**−**D**) and known small-molecule modulators (**0**−**17**) are the same as those in Figure 2. (a) Frequency of activity of bicyclic (light bars) or monocyclic (dark bars) compound classes in chemical-genetic assays. Italicized numbers represent the number of compounds in each group. Smooth curves represent theoretical fits of biological measurement data for bicyclic (brown curve) or monocyclic (green curve) classes. (b) Calculated molecular properties for bicyclic and monocyclic classes with entries expressed as the mean ± SD over all 122 compounds in each class.[13] (c) Forty-dimensional average chemical-genetic fingerprints for bicyclic (brown trace) or monocyclic (green trace) classes, resulting from the multidimensional screen illustrated in Figure 1. All measurements were made in duplicate, and values represent averages over all members (122 compounds; 244 measurements) for each of the two classes. Gray bars indicate assays for which class-average *Z*-scores differ by $>0.5\ \sigma$. (d) Heat-map representation of average chemical-genetic fingerprints for monocyclic and bicyclic classes, depicting both high-signal (red blocks) and low-signal (blue blocks) statistical outliers. (e) Hierarchical clustering (using a linear correlation function) of 12 conformationally distinct categories on the basis of biological measurements, showing both high-signal (red blocks) and low-signal (blue blocks) statistical outliers.[15] Superatoms **R** and $\mathbf{R_1}$ are defined essentially as in Figure 4, with $\mathbf{R_1}$ including the reagents {2−6,8,9}. Each row of blocks represents average scores (24 measurements) for 12 appendage-matched compounds with connectivity and stereochemistry defined as indicated on the dendrogram (**B**/**M**; **dieq**/**diax**; **Glc** = glucose (I), **Gal** = galactose (II), **Man** = mannose (III); see Figure 4).

parts and treated under conditions leading to carbamates or benzoates (Figure 4; **R**). Treatment with $Pd(PPh_3)_4$ and thiosalicylic acid in THF afforded 3,4- or 4,5-diol products quantitatively. Differentially substituted ω-pentenoic acids were coupled to the diols under standard conditions, affording bis-pentenoate products in high purity and yield (Figure 4; $\mathbf{R_1}$). A portion of each of these diesters was subjected to the action of the second-generation Grubbs' catalyst,[10] resulting in bicyclic products in high yield. This library synthesis strategy yields equal numbers of mono- and bicyclic products having twelve distinct stereochemical patterns (Figure 4) resulting from the combination of two (3,4- and 4,5-protected) substitution patterns, three carbohydrate templates, and two α-substitution relationships. This strategy is an illustration of assay measurements guiding the synthesis design; since the objective is to assess the role of stereochemical and skeletal diversity on biological outcomes, we turned to the use of DOS to prepare sets of compounds matched in numbers to their siblings in every respect.

Multidimensional Screening. 244 compounds were used to create a matrix of 19 520 (= 244 × 40 × 2) biological measurements involving 40 parallel cell-based assays. Cell-based assay readouts were chosen to assess broadly the consequences of small-molecule perturbation of mammalian cells and include measurements that report on DNA synthesis,[11a] cellular esterase

(9) (a) Tallarico, J. A.; Depew, K. M.; Pelish, H. E.; Westwood, N, J.; Lindsley, C. W.; Shair, M. D.; Schreiber, S. L.; Foley, M. A. *J. Comb. Chem.* **2001**, *3*, 312−318. (b) See Supporting Information (Section IV) for a detailed description parallel library synthesis.

(10) Scholl, M.; Trnka, T. M.; Morgan, J. P.; Grubbs, R. H. *Tetrahedron Lett.* **1999**, *40*, 2247−2250.

activity,[11b] mitochondrial membrane potential,[11c] and intracellular reducing equivalents.[11d] These four readouts were expanded to 40 cell-based assays, each performed in duplicate, by exposing cells simultaneously to library members and to small molecules of known biological activity (i.e., chemical-genetic modifier screens[6]). A matrix of data was created using 40 (of 72 possible) combinations of the four readouts with 18 different cellular conditions (see Figure 2b). In duplicate experiments, each compound was independently assigned a signed (i.e., "+" or "−") *Z*-score corresponding to the number of standard deviations it fell from the mean of a well-defined mock-treatment distribution. This distribution was determined to be consistent with experimental noise observed under cell-based assay conditions.[5] The resulting collection of continuous-valued *Z*-scores represents the primary dataset used for further analysis. For analyses dependent upon discrete (i.e., binned) outcome states, *Z*-score data were further subjected to a threshold that resulted in each measurement being scored as a high- or low-signal outlier, or as a nonoutlier, from the mock-treatment distribution, based on the probability that the measurement could be explained by assay noise ($P_{noise} < 0.0006$).[5] To reduce further the possibility of false-positive scoring, we required that any compound called a positive be scored as a positive in *both* replicates for a given assay, resulting in an overall average "hit" rate for the binned dataset of less than 1%.

Data Analysis. One of our primary observations was that precursor monocycles (**M**) generally scored as positive in a larger number of the 40 assays than did their bicyclic (**B**) counterparts (Figure 5a). To test the statistical significance of this result, we fit compound Gamma−Poisson model distributions to each dataset and applied a likelihood ratio test for significance.[12] The reported *P*-value ($P < 0.0002$; the probability of observation in a random dataset) was obtained by permutation testing; matched pairs of compounds were randomly assigned labels **B** and **M** (one of each label per pair) before computing the likelihood ratio test on each permuted dataset. For only 11 of more than 89 000 permuted datasets was the likelihood ratio score for randomly permuted data higher than that for the experimental data, indicating that our experimental results are extremely unlikely to have occurred by chance. Overall, this observation suggests that the propensity of these compounds to score frequently as active in multidimensional screening is reduced upon imposition of conformational constraints resulting from the formation of the second ring.

In an attempt to rationalize these results in terms of calculable properties of small molecules, we calculated certain average molecular descriptor values we intuitively thought relevant to conformational restriction, including the number of rotatable bonds, for each of the **M** and **B** compound classes (Figure 5b).[13] These tabular data show that the number of rotatable bonds, of the descriptors computed, are best able to distinguish between the **M** and **B** compound classes, a result reminiscent of a previous report of the importance of this descriptor in predicting oral bioavailability.[14] In that study, limitations on oral bioavailability resulted from the interaction of small molecules with complex biological processes involving numerous metabolic enzymes, a situation comparable to the use of broad cell-based assay measurements, as described herein.

In a preliminary attempt to determine which cell-based assays might best distinguish between the **M** and **B** compound classes, we represented 40-dimensional average chemical-genetic fingerprints[5] both as activity "signatures" (Figure 5c) and as a mathematically equivalent heat map (Figure 5d). In these visualizations, activities are represented as *Z*-scores averaged over all members (and replicates) within the **M** and **B** compound classes. These data represent two different visual approaches to defining assays that discriminate between the two classes. Noting that some assays result in greater variation of data than others, chemical-genetic fingerprints based on a subset of these cell-based assays might be used in future related studies. It is also possible that a subset of these assays might be used as an empirical surrogate for molecular properties related to conformational flexibility (e.g., oral bioavailability).[14]

To expand the scope of our global analysis of the impact of chemical diversity elements on biological outcomes, we prepared average chemical-genetic fingerprints (see Figure 1) for each of six stereochemical categories (for each of the **M** and **B** classes) resulting from the combination of three carbohydrate templates and two α-substitution relationships on the 12-membered rings (or corresponding acyclic chains). To eliminate bias in our analysis introduced by different appendage representations between the categories, only 3,4-bis-pentenoates (and their products) were considered in this analysis, resulting in 12 groups of 12 compounds each having a uniform representation of appendages across all 12 groups. For each of these 12 categories, whose membership was based solely on the chemical diversity elements of interest, average chemical-genetic fingerprints were computed as before, and these fingerprints were hierarchically clustered using linear correlation between fingerprints as a similarity metric (Figure 5e).[15] If categories with a common structural element cluster together based on biological performance, then there exists a correlation between this structural element and global biological outcome. Conversely, if structurally unrelated categories cluster based on performance, there is no such correlation of biological outcome with stereochemical diversity elements. Our observations suggest the former scenario for this dataset. Notably, membership in the **M** or **B** compound class has the dominant overall effect on biological outcome (Figure 5e; similarity < 0.43), extending a less complex result (based on a binary "hit" versus non-"hit" metric; see Figure 5a) to a 40-dimensional biological measurement space. Furthermore, the α-substitution relationship on the 12-membered rings determines subclustering with the **B** class irrespective of carbohydrate template (Figure 5e, top branch of dendrogram; similarity < 0.85). Each of these two subclusters is further divided into *trans*-fused (**Glc**,**Gal**) and *cis*-fused (**Man**) [10.4.0] bicyclic systems. In contrast, subclusters from the **M** class are chiefly determined by the identity of the carbohydrate template itself (Figure 5e, bottom branch of dendrogram; similarity < 0.87).

(11) (a) Stockwell, B. R.; Haggarty, S. J.; Schreiber, S. L. *Chem. Biol.* **1999**, *6*, 71−83. (b) Parish, C. R. *Immunol. Cell. Biol.* **1999**, *77*, 499−508. (c) Wong, A.; Cortopassi, G. A. *Biophys. Res. Commun.* **2002**, *298*, 750−754. (d) Perrot, S.; Duterte-Catella, H.; Martin, C.; Rat, P.; Warnet, J. M. *Toxicol. Sci.* **2003**, *72*, 122−129.

(12) See Supporting Information (Section VI) for a detailed description of the Gamma−Poisson model fit and the likelihood ratio test.

(13) Molecular descriptor values were calculated using Pipeline Pilot (Scitegic, Inc.; San Diego, CA).

(14) Veber, D. F.; Johnson, S. R.; Cheng, H.-Y.; Smith, B. R.; Ward, K. W.; Kopple, K. D. *J. Med. Chem.* **2002**, *45*, 2615−2623.

(15) Hierarchical clustering and data visualization were performed using Spotfire Decision Site 7.0 (Spotfire, Inc.; Somerville, MA).

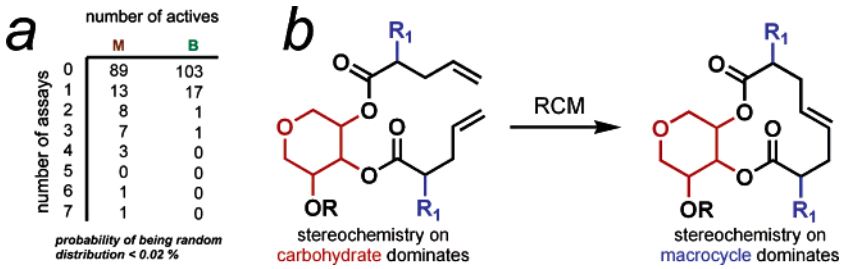

Figure 6. Summary of results interpretation. (a) Table depicting the overall frequencies of activity of monocyclic (**M**) or bicyclic (**B**) compounds in chemical-genetic assays. (b) Dominance of stereochemical features on biological outcomes before and after RCM.

In each of the **M** and **B** compound classes, average chemical-genetic fingerprints for six categories (based on the stereochemistry of the 3-,5-positions of the carbohydrate and the α-position of the appended ester) established the relative importance of diversity elements to different degrees. Our rationale in using *average* chemical-genetic fingerprints across measurements was to augment truly significant values while diminishing the impact of both random and systematic error inherent in the collection of cell-based assay data. Though a smaller number of assays may have sufficed to discriminate between the **M** and **B** compound classes (Figure 5c,d), a substantial fraction (37.5%) of the 40 cell-based assays were necessary to rank stereochemical elements with respect to their association with macrocyclization (data not shown), a substantially richer biological measurement space than would be afforded (10%) using the four cell-based assay readouts alone (i.e., without a chemical-genetic modifier screening strategy). The addition of further orthogonal measurements would likely be necessary to provide significant resolution between additional diversity elements (e.g., appendage-based diversity elements) present in this library of DOS-derived small molecules.

Conclusion

Conformational restriction by macrocyclization has previously been intuited to enhance binding affinity and metabolic stability of the resulting products.[16] Here, we report an experimental demonstration of the effects of macrocyclization and stereochemistry (on both the macroring precursors and the macrorings themselves) using a set of closely related compounds prepared by DOS and a multidimensional chemical-genetic approach. Cyclic connectivity of an otherwise identical compound set significantly influences compound performance in cell-based assays. For example, 17 out of 19 active compounds from the **B** compound class scored as a "hit" in exactly one of 40 assays, whereas more than 60% of active compounds from the **M** compound class scored as a "hit" in two or more assays (Figure 6a). The average activity frequency for active compounds of the **B** class is 1.2 assays per compound, while that of the **M** class is 2.3 assays per compound. Hierarchical clustering (Figure 5e) was further able to resolve this remarkable difference in performance between **M** and **B** compound classes when groups of compounds with common stereochemical elements were taken together. Overall, relationships between stereochemical elements within the **M** and **B** compound classes depends primarily on **M** versus **B** class membership; whereas the stereochemistry of macrocyclic appendages was the dominant determinant for the **B** class, the stereochemistry of the carbohydrate ring itself was the primary determinant for the **M** class in global activity patterns (Figure 6b). These studies illustrate a process for measuring the biological consequences of stereochemical and skeletal diversity in small molecules and small-molecule assays.

Acknowledgment. We gratefully acknowledge John Tallarico and Max Narovlyansky for experimental advice and assistance and Stephen Haggarty and Justin Lamb for helpful comments on the manuscript. We thank the National Institute of General Medical Sciences for support of this research and the National Cancer Institute (NCI), the Keck Foundation, Merck KGaA, and Merck & Co. for support of the Broad Institute Chemical Biology Program (formerly ICCB), and the NCI for support of the Initiative in Chemical Genetics. S.L.S. is an investigator with the Howard Hughes Medical Institute at Harvard University.

Note Added after ASAP Publication: This article was published on the Web 10/20/2004 with minor errors in refs 9 and 11. The correct version posted 10/28/2004 and the print version are correct.

Supporting Information Available: General experimental procedures, spectral characterization data, assay protocols, assay data, and data analysis methods. This material is available free of charge via the Internet at http://pubs.acs.org.

JA048170P

(16) Burger, M. T.; Bartlett, P. A. *J. Am. Chem. Soc.* **1997**, *119*, 12697−12698 and references therein.